Journal of Inorganic and General Chemistry
ZAAC
Zeitschrift für anorganische und allgemeine Chemie
www.zaac.wiley-vch.de
RESEARCH ARTICLE
DOI: 10.1002/zaac.202200266

Synthesis and Crystal-Structure Analysis of the K_2NiF_4-Type Hydride Oxides $LiLnEuH_{2-x}O_2$ (*Ln* = La, Ce, Pr, Nd, Sm) and $LiEu_2H_3O$ by Neutron and X-Ray Diffraction

Jean-Louis Hoslauer,[a] Nicolas Zapp,[b] Henry E. Fischer,[c] Daniel Rudolph,[a] Holger Kohlmann,*[b] and Thomas Schleid*[a]

Dedicated to Professor Wolfgang Schnick on the Occasion of his 65th Birthday

The hydride oxides $LiLnEuH_{2-x}O_2$ (*Ln* = La, Ce, Pr, Nd and Sm) were synthesized by reaction of the lanthanide sesquioxides with europium monoxide, europium dihydride and lithium hydride under inert conditions at 750 °C as black powders. They crystallize in the tetragonal K_2NiF_4-type structure (space group: *I*4/*mmm*) with a mixed Ln^{3+}/Eu^{2+} occupation. The crystal structures of the europium representatives $LiLaEuH_{2-x}O_2$ and $LiLaEuD_{2-x}O_2$ were analyzed by powder neutron diffraction data at short wavelengths (λ = 70 pm). Hydrogen (deuterium) and oxygen atoms occupy distinct crystallographic sites with considerable vacancy concentrations on the hydrogen positions (a = 363.80(8) pm, c = 1323.3(3) pm, c/a = 3.637 for $LiLaEuH_{1.26(4)}O_2$ and a = 363.43(5) pm, c = 1321.6(2) pm, c/a = 3.636 for $LiLaEuD_{1.41(2)}O_2$). Moving from the mixed *Ln*/Eu occupation in $LiLnEuH_2O_2$ to *Ln* = Eu^{2+}, we obtained the mixed-anionic phase $LiEu_2H_3O$, which crystallizes in the same structure type with a = 370.04(2) pm, c = 1317.32(8) pm and c/a = 3.560.

Introduction

In 1962, *Carter* reported on a new class of compounds with the composition *Ln*HO (*Ln* = La, Ce and Pr).[1] At first glance, the presence of both hydrogen and oxygen atoms may falsely lead to the conclusion that it contains hydroxide anions (OH^-). As it could be shown through neutron diffraction experiments,[2] the hydrogen is present as a hydride anion (H^-), so *Ln*HO (*Ln* = La, Ce and Pr) were thus the first examples of rare-earth metal hydride oxides (also known as 'oxyhydrides'). Over time, further rare-earth metal hydride oxides *Ln*HO were synthesized and characterized, including the lanthanoids *Ln* = Nd,[3] Sm,[4,5] Gd,[4,6] Tb,[4] Dy,[4,7] Ho,[4,8] Er,[4,7] Lu[7] and Y.[9,10]

Moving from ternary to quaternary compounds by reacting rare-earth metal sesquioxides (Ln_2O_3: *Ln* = La–Nd) with an excess of lithium hydride (LiH) in a lithium-chloride flux (LiCl), hydride oxides of the composition $LiLn_2HO_3$ (*Ln* = La–Nd) can be obtained.[11] Although containing basic hydride anions, these compounds show a remarkable stability against water as the flux can be removed using demineralized water.[11] With the isotypic Sr_2LiH_3O, $LiLa_2HO_3$ forms solid solutions of the composition $La_{2-x-y}Sr_{x+y}LiH_{1-x+y}O_{3-y}$ ($0 \le x \le 1$; $0 \le y \le 2$; $0 \le x+y \le 2$) with K_2NiF_4-type structures. Compounds from this series showed pure hydride-ion conduction, *i.e.* without simultaneous electronic conduction, for the first time.[12] Because of their potential use in energy storage and conversion, this discovery has triggered research in the field of rare-earth metal hydride oxides considerably. The idealized stoichiometric composition $LiLaSrH_2O_2$ served as inspiration for an all-lanthanide derivative of the same composition, exchanging Sr^{2+} for the almost identically sized Eu^{2+} cation. By reaction of La_2O_3, EuH_2, EuO and LiH, the hydride oxide $LiLaEuH_2O_2$ was formed and by single-crystal X-ray diffraction experiments a tetragonal K_2NiF_4-type structure was assigned.[13] Because of the close positions of lanthanum and europium in the periodic table of the elements and the low scattering contribution of hydrogen, questions of La/Eu and H/O atomic order in the crystal structure could not be resolved reliably.[13] This is why neutron diffraction was employed in this study. While the hydride and oxide anions in the $LiLn_2HO_3$ phases are well ordered,[11] a mixed occupation, *i.e.* H/O disorder, was reported for $La_{2-x-y}Sr_{x+y}LiH_{1-x+y}O_{3-y}$ ($0 \le x \le 1$; $0 \le y \le 2$; $0 \le x+y \le 2$).[12] Hydride-anion conductivity is strongly influenced by the degree of H/O order, which is why such studies are of importance in the investigation of hydride oxides.[14] Due to the increased scattering contrast between light elements like hydrogen, lithium and oxygen towards heavy elements like lanthanum and europium (b_c in fm: −3.74 (H), 6.67 (D), 5.80 (O), 8.24 (La), 7.22 (Eu)[15]), neutron diffraction

[a] J.-L. Hoslauer, Dr. D. Rudolph, Prof. Dr. T. Schleid
Institute for Inorganic Chemistry, University of Stuttgart
Pfaffenwaldring 55, 70569 Stuttgart, Germany
E-mail: schleid@iac.uni-stuttgart.de
[b] Dr. N. Zapp, Prof. Dr. H. Kohlmann
Institute for Inorganic Chemistry, Leipzig University
Johannisallee 29, 04103 Leipzig, Germany
E-mail: holger.kohlmann@uni-leipzig.de
[c] Dr. H. E. Fischer
Institute Laue-Langevin, 71 avenue des Martyrs,
CS 20156, 38042 Grenoble cedex 9, France

Supporting information for this article is available on the WWW under https://doi.org/10.1002/zaac.202200266

is a suitable tool for this task. Furthermore, neutron scattering is isotope sensitive. For this reason, a combined refinement on diffraction data of a hydride and the corresponding deuteride with constrained occupation factors of hydrogen and deuterium atoms can increase the accuracy of the crystal structure. Due to the high absorption of thermal neutrons by ^{nat}Eu samples, neutron diffraction on europium containing specimen affords either the use of isotopically enriched material, or the measurement at the absorption minimum with short wavelength monochromatic neutron radiation, at the cost of a decreased angular resolution.[16]

Results and Discussions

The reaction of lanthanide sesquioxides, europium monoxide, europium dihydride and lithium hydride under inert conditions at 750 °C yielded the hydride oxides Li*Ln*EuH$_2$O$_2$ (*Ln* = La, Ce, Pr, Nd and Sm) as black powders. They are stable in air for a prolonged time and slowly decompose after months upon exposure to humid air. Samples that have been submerged in water for a few hours only showed minimal decay. For the composition LiLaEuH$_2$O$_2$ the cystal structure was solved and refined in the tetragonal K$_2$NiF$_4$-type structure from single-crystal diffraction data (Table 1). The crystal structures of further isotypic compounds were refined based on powder X-ray diffraction (PXRD, Table 2). Additionally, the reaction of EuO, EuH$_2$ and LiH yielded single crystals of LiEu$_2$H$_3$O together with several side-phases. The crystal structures of LiEu$_2$H$_3$O and LiSr$_2$H$_3$O are isotypic as determined by single-crystal X-ray diffraction.[12] Europium shows an X-ray absorption edge (L_{III}) close to the K_α emission of copper X-ray tubes,[17] yielding high background due to fluorescence. A powder X-ray diffractometer using a molybdenum anode was thus used to avoid this problem. As expected, these laboratory-based powder X-ray diffraction data neither allowed for a clear distinction between *Ln* (= La, Ce, Pr, Nd, Sm) and europium atoms, nor for an accurate localization of the hydrogen atoms. Even from single-crystal X-ray diffraction data[13] the question of *Ln*/Eu and H/O atomic order could not be solved reliably.

In order to shed more light on the question of order *versus* disorder in the crystal structure of LiLaEuH$_2$O$_2$, neutron diffraction experiments were performed. This was complicated in the present case by a number of peculiarities of the samples. Due to its large incoherent scattering cross section, resulting in high scattering background, hydrogen is often substituted by deuterium for neutron diffraction. The scattering contrast between deuterium and oxygen atoms, however, is much smaller than between hydrogen (natural isotopic mixture) and oxygen atoms (bound coherent neutron scattering lengths b_c in fm: −3.74 (H), 6.67 (D), 5.80 (O), 8.24 (La), 7.22 (Eu)[15]). Therefore, both the hydride LiLaEuH$_2$O$_2$ and the deuteride LiLaEuD$_2$O$_2$ were investigated by neutron diffraction. In order to compensate for the high background in the hydride case, a high-flux neutron source is needed. Furthermore, the high neutron absorption of europium samples usually prevents their study by neutron diffraction. This can be circumvented by using neutrons of short wavelength, as the neutron absorption of the natural isotope mixture of europium, ^{nat}Eu, exhibits a minimum at λ = 70 pm,[16] at the cost of a reduced angular resolution. Both

Table 1. Crystallographic data for the single-crystal X-ray structure refinement of LiLaEuH$_2$O$_2$.

Formula	LiLaEuH$_2$O$_2$
Space group	*I*4/*mmm* (no. 139)
Crystal system	tetragonal
a/pm	363.96(2)
c/pm	1320.74(8)
c/*a*	3.629
Formula units, *Z*	2
Calculated density, D_x/g cm^{-3}	6.299
Molar volume, V_m/cm^3 mol^{-1}	52.68 (1)
Diffractometer	κ-CCD (Bruker-Nonius)
Radiation	Mo-K$_\alpha$ (λ = 71.09 pm)
$2\Theta_{max}$/°	55.69
F(000)	282
Range, ±*h*, ±*k*, ±*l*	4, 4, 16
Abs. coefficient, μ/mm^{-1}	29,57
Meas./symm. ind. reflections	931/87
R_{int}/R_σ	0.051/0.021
R_1 for *n* refl. with $\lvert F_o \rvert \geq 4\sigma(F_o)$	0.013 for *n* = 87
R_1/wR_2 for all reflections	0.013/0.029
Structure solution and refinement	SHELX [33]
Goodness of Fit	1.121
Res. elec. dens., $\rho_{max/min}$/e$^-$ Å^{-3}	0.57/−0.80
CSD number	433587

Table 2. Lattice parameters of the Li*Ln*EuH$_2$O$_2$ representatives (*Ln* = Ce, Pr, Nd and Sm) with K$_2$NiF$_4$-type structure, space group: *I*4/*mmm* (no. 139).

Compound	*a*/pm	*c*/pm	*c*/*a*
LiCeEuH$_2$O$_2$	362.117(1)	1314.228(6)	3.629
LiPrEuH$_2$O$_2$	360.477(2)	1307.860(8)	3.628
LiNdEuH$_2$O$_2$	358.904(3)	1303.069(15)	3.631
LiSmEuH$_2$O$_2$	357.805(4)	1299.200(16)	3.631

Table 3. Refined crystallographic data for LiLaEuH$_{1.26(4)}$O$_2$ based on neutron powder diffraction data at ambient temperature.

Formula	LiLaEuH$_{1.26(4)}$O$_2$
Space group	*I*4/*mmm* (no. 139)
Crystal system	tetragonal
a/pm	363.80(8)
c/pm	1323.3(3)
c/*a*	3.637
Formula units, *Z*	2
Calculated density, D_x/g cm^{-3}	6.278
Molar volume, V_m/cm^3 mol^{-1}	52.74(1)
Diffractometer	D4 [18]
Radiation	Neutrons, λ_n = 69.42 pm
2Θ range/°	1.7–137.9
Structure refinement	FullProf [34]
$R_p/R_{wp}/R_{exp}$	1.42 %/1.85 %/1.97 %
X^2/R_B	0.89/7.03 %
CSD number	2164837

Journal of Inorganic and General Chemistry
ZAAC
Zeitschrift für anorganische und allgemeine Chemie

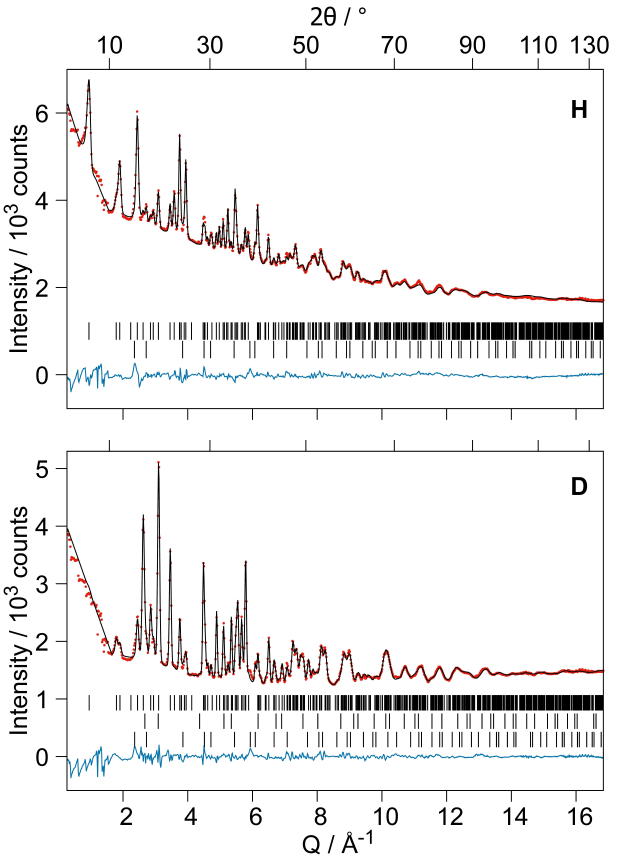

Figure 1. *Rietveld* refinement of the crystal structures of $LiLaEuH_{1.26(4)}O_2$ (**H**, top) and $LiLaEuD_{1.41(2)}O_2$ (**D**, bottom) based on neutron-diffraction data at ambient temperature (D4 diffractometer, $\lambda_n = 69.42$ pm, doi:10.5291/ILL-DATA.5-22-775). **H**: $R_{wp} = 1.85\,\%$, $GoF = 0.94$. Bragg markers denote from top to bottom: $LiLaEuH_{1.26(4)}O_2$ (*I*4/*mmm*, 97(2) wt.%, $R_I = 7.0\,\%$, $a = 363.80(8)$ pm, $c = 1323.3(3)$ pm, in orange), Li_2O (*Fm*$\bar{3}$*m*, 2.28(13) wt.%, $a = 462.52(19)$ pm, in purple). **D**: $R_{wp} = 2.63\,\%$, $GoF = 1.08$. *Bragg* markers denote from top to bottom: $LiLaEuD_{1.41(2)}O_2$ (*I*4/*mmm*, 98(2) wt.%, $R_I = 4.3\,\%$, $a = 363.43(5)$ pm, $c = 1321.6(2)$ pm, in orange), LiD (*Fm*$\bar{3}$*m*, 0.12(2) wt.%, $a = 407.2(4)$ pm, in purple), Li_2O (*Fm*$\bar{3}$*m*, 1.95(10) wt.%, $a = 461.79(15)$ pm, in green). Black curve: measurement, red curve: simulation, blue curve: difference. Mind the different x scaling of the individual graphs.

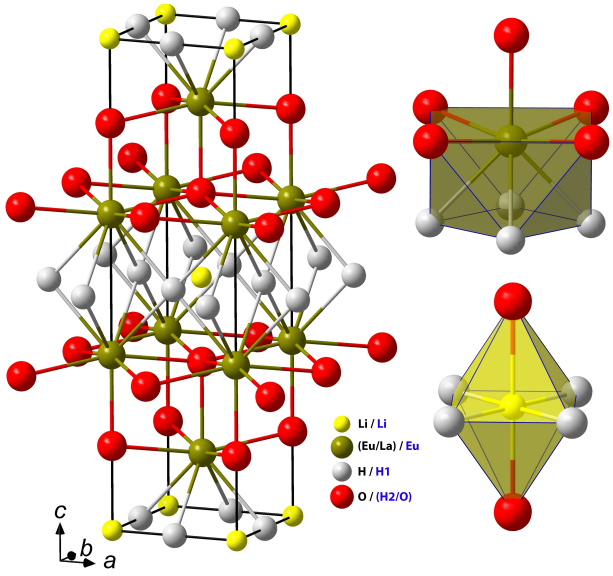

Figure 2. Crystal structure of $LiLaEuH_2O_2$ and $LiEu_2H_3O$ (left) with coordination polyhedra of the cations (right). The atom types are labelled in black for $LiLaEuH_2O_2$ and in blue for $LiEu_2H_3O$.

Table 4. Refined crystallographic data of $LiLaEuD_{1.41(2)}O_2$ based on neutron powder diffraction data at ambient temperature.

Formula	$LiLaEuD_{1.41(2)}O_2$
Space group	*I*4/*mmm* (no. 139)
Crystal system	tetragonal
a/pm	363.43(5)
c/pm	1321.6(2)
c/*a*	3.636
Formula units, *Z*	2
Calculated density, D_x/g·cm^{-3}	6.327
Molar volume, V_m/cm^3·mol^{-1}	52.86(1)
Diffractometer	D4, ILL [18]
Radiation	Neutrons, $\lambda_n = 69.42$ pm
2Θ range/°	1.7–137.9
Structure refinement	FullProf [36]
$R_p/R_{wp}/R_{exp}$	1.67 %/2.63 %/2.43 %
χ^2/R_B	1.17/4.36 %
CSD number	2164838

$$R_p = \left(\frac{\sum_i |y_i - y_{calc,i}|}{\sum_i y_i}\right) \cdot 100\,\%,\ R_{wp} = \sqrt{\frac{\sum_i w_i |y_i - y_{calc,i}|^2}{\sum_i w_i \cdot y_i^2}} \cdot 100\,\%,$$

$$R_{exp} = \sqrt{\frac{n-p}{\sum_i w_i \bullet y_i^2}} \cdot 100\,\%,\ \chi^2 = \left(\frac{R_{wp}}{R_{exp}}\right)^2,\ R_B = \frac{\sum_h |I_h - I_{calc,h}|}{\sum_h |I_h|} \cdot 100\,\%$$

requirements are met by the D4 diffractometer at the *Institute Laue-Langevin* (ILL) in Grenoble (France).[18]

The Rietveld refinement of the crystal structures of $LiLaEuH_2O_2$ and $LiLaEuD_2O_2$ based on neutron-diffraction data confirmed the K_2NiF_4-type structure (Figures 1 and 2, Tables 3–6). Hydrogen (deuterium) and oxygen atoms are found on distinct crystallographic sites 4*c* and 4*e* without significant mixing, whereas the related $LiSrLaH_2O_2$ compound shows a small amount of H/O mixing on the 4*c* site[19] The latter was determined on XRD data only, though.

The Li–H, Li–D, and Li–O distances (Table 7) are similar to those in $LiLa_2HO_3$ (Li–H: 179 pm, Li–O: 229 pm[20]) and $LiSrLaH_2O_2$ (Li–H: 182 pm, Li–O: 228 pm[19]), but smaller than those in the binary lithium compounds (LiH, LiD: 203 pm, 204 pm;[21,22] Li_2O: 200 pm[22]). The La–H/D and Eu–H/D distances (Table 6) are nearly identical to those in $LiSrLaH_2O_2$ (264 pm[19]) and slightly larger than in $LiLa_2HO_3$ (258 pm[20]), which reflects the larger ionic radius of Eu^{2+} *resp.* Sr^{2+} compared to La^{3+}.[23] They are also similar to those in salt-like europium(II) deuterides (EuD_2: 238–276 pm; $LiEuD_3$: 268 pm,[24] $EuMg_2D_6$: 254–263 pm[25]). The La–O and Eu–O distances (Table 6) resemble those in $LiLa_2HO_3$ and $LiSrLaH_2O_2$ (243 pm[20] and 245 pm[19]), but are smaller than in *C*-type Eu_2O_3 (240–239 pm[26]) and much larger than in NaCl-type EuO (207 pm[27]).

Table 5. Atomic positions, site occupation factors, anisotropic and equivalent isotropic displacement parameters (U_{ij}/U_{eq} [a] in pm^2) for the crystal structure of $LiLaEuH_2O_2$ as determined by single-crystal X-ray diffraction.

Atom	Site	*s.o.f.*	*x/a*	*y/b*	*z/c*	U_{11}	U_{33}	U_{eq}
Li	2*a*	1	0	0	0	95(52)	202(107)	131(36)
La	4*e*	0.5	0	0	0.35669(2)	75(3)	60(4)	70(3)
Eu	4*e*	0.5	0	0	*z*(La)	U_{11}(La)	U_{33}(La)	U_{eq}(La)
H	4*c*	1	0	$^1/_2$	0	–	–	210[b]
O	4*e*	1	0	0	0.1719(6)	128(9)	194(27)	150(12)

[a] $U_{eq} = {}^1/_3\,[U_{11} + U_{22} + U_{33}]$, [b] the isotropic displacement parameter of the H atom was constrained to the La/Eu site according to $U_{eq}(H) = 3\,U_{eq}(La/Eu)$.

Table 6. Atomic positions in the crystals structures of $LiLaEuH_{1.26(4)}O_2$ (**H**) and $LiLaEuD_{1.41(2)}O_2$ (**D**) based on NPD measurements at ambient temperature.

Atom	Site	*s.o.f.*		*x/a*	*y/b*	*z/c*		$B_{iso}/10^{-4}$ pm^2	
		H	**D**			**H**	**D**	**H**	**D**
Li	2*a*	1		0	0	0	0	0.8(2)	0.8(2)
La	4*e*	0.5		0	0	0.3572(2)	0.35715(19)	0.28(5)	0.19(3)
Eu	4*e*	0.5		0	0	*z*(La)	*z*(La)	B_{iso}(La)	B_{iso}(La)
H/D	4*c*	0.63(2)	0.703(12)	0	$^1/_2$	0	0	0.51(15)	0.80(6)
O	4*e*	1		0	0	0.1723(3)	0.1729(2)	0.72(6)	1.55(10)

Table 7. Interatomic distances (*d*/pm) up to 300 pm in $LiLaEuH_{1.26(4)}O_2$ (**H**) and $LiLaEuD_{1.41(2)}O_2$ (**D**).

Atom 1	Atom 2	Multiplicity	*d*/pm	
			H	**D**
Li	H/D	4	181.90(4)	181.72(3)
Li	O	2	228.0(4)	228.5(3)
La/Eu	H/D	4	262.29(19)	262.03(18)
La/Eu	O	1	244.7(5)	243.5(4)
La/Eu	O	4	260.19(7)	260.03(6)
O	H/D	4	291.7(3)	291.9(2)
H/D	H/D	4	257.25(6)	256.98(4)

The isotropic displacement parameters of the Li, La, Eu and D atoms resemble those in related heteroanionic hydrides (B_{iso} in 10^{-4} pm^2: 0.65 (Li),[11] 0.4–0.5 (La)[11,19,20]), 0.6–0.7 (O),[11,19,20] 1.5 (D)[11]), although that of hydrogen is rather small. This small B_{iso} value of hydrogen atoms resembles that one in other hydride oxides, *e.g.* LaHO (0.4 10^{-4} pm^2[2]) and it is smaller than the value of deuterium, which seems to contrast the expectations of an isotope effect. The isotope effect is clearly seen in the lattice parameters and interatomic Li–H/D and La/Eu–D distances, which are slightly smaller for the deuteride (Table 6) as compared to the hydride.

Both hydride and deuteride show a remarkably high vacancy concentration on the hydrogen *resp.* deuterium site, which is why the refined empirical formulae considerably deviate from the nominal ones: $LiLaEuH_{1.26(4)}O_2$ and $LiLaEuD_{1.41(2)}O_2$. Such vacancies were observed for isotypical K_2NiF_4-type hydrides before[11,12] and are substantial for the hydride-anion conductivity[28,29] which was recently reported for several representatives.[12,20,28,30–32] A deeper understanding for the formation of hydrogen defects, as well as the analysis and control of their concentration is therefore pivotal for the study of hydride conductivity in these compounds. The oxygen site does not exhibit significant vacancy concentrations in both cases and the La/Eu ratio does not deviate significantly from 1, which is why the occupancy factors of all three elements were fixed in the refinement. When the refined unit-cell parameters of $LiLaEuH_2O_2$ are compared with the other hydride oxides of the composition $LiLnEuH_2O_2$, a decrease in both the *a* and the *c* axes is observed from the larger La^{3+} towards the smaller Sm^{3+} cation as consequence of the lanthanoid contraction, maintaining the *c*/*a* ratio.

The structure of $LiEu_2H_3O$ could only be refined from single-crystal X-ray diffraction data (Tables 8–10). Here, $LiLaEuH_2O_2$ shows a smaller cell volume as the lattice parameter *a* is larger in $LiEu_2H_3O$, while the *c* axis appears slightly smaller. The expansion of the *a* axis could be explained with the increase of the ionic radius, when the smaller La^{3+} is replaced with the larger Eu^{2+} cation. While the mixed La/Eu 4*e* site in $LiLaEuH_2O_2$ becomes fully occupied by Eu^{2+} in $LiEu_2H_3O$, the oxide position now shows a mixed-anionic site with H and O (Table 9). The Li–H1 distances are thus slightly longer in $LiEu_2H_3O$ than in $LiLaEuH_2O_2$, while the Li–H2/O distances are shorter. Similarly, the Eu–H1 distances are shorter in $LiEu_2H_3O$ than the La/Eu–H values in $LiLaEuH_2O_2$, while all Eu–H2/O distances are longer (Table 10). $LiLaEuH_2O_2$ and $LiLaEuD_2O_2$ as well as $LiEu_2H_3O$ (Table 9) crystallize in the tetragonal space group *I*4/*mmm* with the K_2NiF_4-type structure. The rare-earth metal cation sites are surrounded by five oxide (or five mixed ligands) and four hydride anions forming a capped square antiprism $[(La/Eu)H_4O_5]^{12.5-}$ or $[Eu(H1)_4(O/H2)_5]^{9.5-}$, while the lithium cations reside in $[LiH_4O_2]^{7-}$ or $[Li(H1)_4(O/H2)_2]^{6-}$ octahedra. The hydride anions are located in $[HLi_2(La/Eu)_4]^{11+}$ or $[(H1)Li_2Eu_4]^{9+}$ octahedra, while the oxide anions and the mixed anionic sites form $[OLi(La/Eu)_5]^{11.5+}$ and $[(H2/O)LiEu_5)^{+9.5}$ octahedra.

Table 8. Crystallographic data for the single-crystal X-ray structure refinement of $LiEu_2H_3O$.

Formula	$LiEu_2H_3O$
Space group	*I*4/*mmm* (no. 139)
Metrics	tetragonal
a/pm	370.04(2)
c/pm	1317.32(8)
c/*a*	3.560
Formula units, *Z*	2
Calculated density, D_x/g·cm^{-3}	6.074
Molar volume, V_m/cm^3·mol^{-1}	54.31(1)
Diffractometer	κ-CCD (*Bruker-Nonius*)
Radiation	Mo-K_α (λ = 71.09 pm)
$2\Theta_{max}$/°	54.91
F(000)	280
Range, ±*h*, ±*k*, ±*l*	4, 4, 16
Abs. coefficient, μ/mm^{-1}	34.19
Meas./symm. ind. reflections	1708/86
R_{int}/R_σ	0.075/0.021
R_1 for *n* refl. with $\lvert F_o\rvert \geq 4\sigma(F_o)$	0.009 for *n* = 84
R_1/wR_2 for all reflections	0.010/0.018
Structure solution and refinement	SHELX [33]
Goodness of Fit	1.030
Res. elec. dens., $\rho_{max/min}$/e$^-$ Å^{-3}	0.65/−0.83
CSD number	433587

Conclusions

$LiLaEuD_2O_2$ and the hydride oxides $LiLnEuH_2O_2$ (*Ln* = La–Nd and Sm) were synthesized by solid-state reactions of Ln_2O_3 with EuO, EuH_2 (EuD_2) and LiH (LiD). Their crystal structure was determined from single-crystal X-ray diffraction data for $LiLaEuH_2O_2$ and refined from neutron powder diffraction data for *Ln* = La. They crystallize in the tetragonal K_2NiF_4-type structure. In $LiLaEuH_2O_2$ hydride and oxide anions are ordered, while the lanthanum and europium cations share on crystallographic position with a statistical distribution. Neutron powder diffraction revealed a considerable amount of hydride/deuteride vacancies giving the formula $LiLaEuH_{1.26(4)}O$ and $LiLaEuD_{1.41(2)}O$. The hydride/deuteride deficit hints at a possible hydride-anion conductivity that should be further investigated in the future. Using X-ray powder diffraction refinement, the smaller lanthanoid derivatives of the composition $LiLnEuH_2O_2$ (*Ln* = Ce–Nd, Sm) could be characterized as well. Here a decrease in all unit-cell parameters could be observed with a shrinking Ln^{3+}-cation radius. Additionally, the crystal structure of K_2NiF_4-type $LiEu_2H_3O$ was solved and refined from single crystal diffraction data. In contrast to $LiLnEuH_2O_2$, however, it shows an H/O mixed anionic site.

Table 10. Interatomic distances (*d*/pm) up to 300 pm in $LiEu_2H_3O$.

Atom 1	Atom 2	Multiplicity	*d*/pm
Li	H1	4	185.02(1)
Li	H2/O	2	223.3(8)
Eu	H1	4	261.29(2)
Eu	H2/O	1	250.9(8)
Eu	H2/O	4	264.5(1)
H2/O	H1	4	290.0(6)
H1	H1	4	261.66(1)

Experimental Section

The hydride (and deuteride) oxides of the composition $LiLnEuH_2O_2$ (*Ln* = La–Nd, Sm) were prepared from the corresponding rare-earth metal sesquioxides (1 eq.), europium(II) oxide EuO (1 eq.), europium(II) hydride EuH_2 or europium(II) deuteride EuD_2 (1 eq.) and an excess of lithium hydride LiH (2 eq.) in evacuated, silica-jacketed, arc-welded niobium capsules under helium atmosphere (800 mbar) at 750 °C for 72 h. Single crystals of $LiEu_2H_3O$ were prepared in a similar manner by reacting EuH_2 (1 eq.), EuO (1 eq.) and an excess of LiH (2 eq.) under the same conditions.

La_2O_3 (99.99% *ChemPur*, Karlsruhe), Nd_2O_3 (99.99% *ChemPur*, Karlsruhe), Sm_2O_3 (99.99% *ChemPur*, Karlsruhe) and LiH (99.4% *Alfa Aesar*, Karlsruhe) were obtained commercially Ce_2O_3 and Pr_2O_3 were prepared from CeO_2 (99.9% *ChemPur*, Karlsruhe) and Pr_6O_{11} (99.9% *ChemPur*, Karlsruhe) with the corresponding metals Ce (99.9% *ChemPur*, Karlsruhe) and Pr (99.9% *ChemPur*, Karlsruhe) at 1100 °C for 120 h in sealed niobium capsules. EuH_2 and EuD_2 were prepared by reacting elemental europium (99.99% *SmartElements*, Vienna) with hydrogen (*Air Liquide*, 99.9%) and deuterium (*Air Liquide*, 99.8%) in home-built inconel autoclaves with copper sealings. The samples were subjected to 6–10 MPa gas pressures and annealed at 400 °C for 72 h. Europium(II) oxide EuO was prepared from EuH_2 and Eu_2O_3 (99.99% *ChemPur*, Karlsruhe) in niobium capsules at 900 °C for 72 h. To prevent possible hydride contaminations in the deuterated sample, $LiLaEuD_2O_2$ was prepared using EuO that was synthesized using EuD_2 and Eu_2O_3.

Neutron diffraction was carried out at the *Institute Laue-Langevin* (ILL, Grenoble, France) at the D4 diffractometer.[18] The samples were finely ground and filled into vanadium cylinders (5 mm diameter) for neutron diffraction (λ_n = 69.42 pm, Cu-220 monochromator). The standard data corrections for intensity normalization, sample attenuation, and geometric aberrations were employed[35] for the here presented diffraction patterns. X-ray powder diffraction samples were finely ground inside an argon-filled glove box and

Table 9. Atomic positions, site occupation factors, anisotropic and equivalent isotropic displacement parameters (U_{ij}/U_{eq}[a] in pm^2) in the crystal structure of $LiEu_2H_3O$ as determined by single-crystal X-ray diffraction.

Atom	Site	*s.o.f.*	*x*/*a*	*y*/*b*	*z*/*c*	U_{11}	U_{33}	U_{eq}
Li	2*a*	1	0	0	0	149(44)	268(65)	189(29)
Eu	4*e*	1	0	0	0.35994(2)	172(2)	141(2)	162(2)
H1	4*c*	1	0	0	0	–	–	243[b]
H2	4*e*	0.509(12)	0	$^1/_2$	0.1695(6)	–	–	202[b]
O	4*e*	0.491(12)	0	0	*z*(H2)	–	–	U_{eq}(H2)

drifted onto *Mylar*® foil (*Chemplex*, Palm City, Florida, U.S.A.) covered with dried high-temperature vacuum grease (*Apiezon*, Manchester, U.K.). Powder patterns were taken on a *Stoe Stadi-P* (*Stoe&Cie*, Karlsruhe) powder diffractometer using Ge-(111)-monochromatized Mo-$K_{\alpha1}$ radiation in transmission mode.

The X-ray and neutron-powder diffraction data were analyzed by the *Rietveld* method[36] using the *FullProf* software package.[34] In refinements on XRPD data half width (*Cagliotti* formula), cell parameters, and asymmetry parameters were refined and the axial divergence was corrected. However, it was not possible to also refine the *Lorentzian* isotropic strain parameter *X*. The isotropic *Debye-Waller* factors (B_{iso}) and the *z*-coordinate were refined for La/Eu and O only. For the hydride and oxide anions a full occupation of the site was kept, according to the starting model from single-crystal refinement. The refined data can be found in the Supporting Information.

For the powder X-ray diffraction data a measured profile was refined using a pseudo-*Voigt* (*pV*) function with additional axial divergence asymmetry correction according to *Finger*, *Cox* and *Jephcoat*.[38,39] This was necessary as the laboratory X-ray powder diffractometer, operating in transmission mode, was not equipped with a *Soller* slit and therefore a strong axial divergence at low angles is typically observed. For the thin layer of drifted powder sample on *Mylar*® foil the absorption of the sample was estimated to be negligible using the X-ray absorption calculator by *Argonne National Laboratories*. For the refinements of the *Ln* = Ce–Nd, Sm derivatives only the isotropic *Debye-Waller* factors (B_{iso}) of the two sites with the highest electron density were considered.

The background of the neutron-diffraction data was fitted by linear interpolation of one point with fixed height and nine points with refineable intensities. The profiles were described with empirical pseudo-*Voigt* functions and three *Cagliotti* parameters (*U*, *V*, *W*), whereas the calculation range was set to 8 times the full width at half maximum. Additionally, the zero-point error, scaling factors, lattice parameters, atomic positions and isotropic thermal displacement parameters B_{iso} were refined for the major phase, and the two first mentioned for the secondary phases. The neutron scattering length of ^{nat}Eu ($b_c = 5.54$ fm for a neutron energy $E = 170$ meV corresponding to the used neutron wavelength of $\lambda = 69.42$ pm) was obtained from tabulated literature data.[37]

Acknowledgements

We acknowledge the *Institute Laue-Langevin* (ILL Grenoble, France) for the provision of beam time at the D4 powder diffractometer (Kohlmann, Cuello, Fischer, Hoslauer, Rudolph, Zapp, Schleid, 2020; doi:10.5291/ILL–DATA.5-22-775). This work was funded by the Deutsche Forschungsgemeinschaft (DFG, German Research Foundation) – Grants 419433503 (KO1803/12-1) and INST 268/379/1 FUGG. Open Access funding enabled and organized by Projekt DEAL.

Data Availability Statement

The data that support the findings of this study are available from the corresponding author upon reasonable request.

Conflict of Interest

The authors declare no conflict of interest.

Keywords: neutron and X-ray diffraction · europium · lanthanides · hydride and deuteride oxides · lithium salts

[1] F. L. Carter, in: *Rare Earth Research* (J. F. Nachman, C. E. Lundin, Eds.), Plenum Press, New York **1961**, 311–320.
[2] B. Malaman, J. F. Brice, *J. Solid State Chem.* **1984**, *53*, 44–54.
[3] M. Widerøe, H. Fjellvåg, T. Norby, F. W. Poulsen, R. W. Berg, *J. Solid State Chem.* **2011**, *184*, 1890–1894.
[4] H. Yamashita, T. Broux, Y. Kobayashi, F. Takeiri, H. Ubukata, T. Zhu, M. A. Hayward, K. Fujii, M. Yashima, K. Shitara, A. Kuwabara, T. Murakami, H. Kageyama, *J. Am. Chem. Soc.* **2018**, *140*, 11170–11173.
[5] N. Zapp, H. Kohlmann, *Z. Naturforsch.* **2018**, *73b*, 535–538.
[6] J. Ueda, S. Matsuishi, T. Tokunaga, S. Tanabe, *J. Mater. Chem.* **2018**, *C 6*, 7541–7548.
[7] N. Zapp, D. Sheptyakov, H. Kohlmann, *Crystals* **2021**, *11*, 750.
[8] N. Zapp, D. Sheptyakov, A. Franz, H. Kohlmann, *Inorg. Chem.* **2021**, *60*, 3972–3979.
[9] J. Montero, F. A. Martinsen, M. García-Tecedor, S. Zh. Karazhanov, D. Maestre, B. Hauback, E. S. Marstein, *Phys. Rev.* **2017**, *B 95*, 201301–201304.
[10] N. Zapp, H. Auer, H. Kohlmann, *Inorg. Chem.* **2019**, *58*, 14635–14641.
[11] H. Schwarz, *Dissertation*, University of Karlsruhe, **1991**.
[12] G. Kobayashi, Y. Hinuma, S. Matsuoka, A. Watanabe, M. Iqbal, M. Hirayama, M. Yonemura, T. Kamiyama, I. Tanaka, R. Kanno, *Science* **2016**, *351*, 1314–1317.
[13] D. Rudolph, *Dissertation*, University of Stuttgart, **2018**.
[14] H. Nawaz, F. Takeiri, A. Kuwabara, M. Yonemura, G. Kobayashi, *Chem. Commun.* **2020**, *56*, 10373–10376.
[15] V. F. Sears, *Neutron News* **1992**, *3*, 26–37.
[16] H. Kohlmann, *Eur. J. Inorg. Chem.* **2010**, 2582–2593.
[17] E. Prince (Ed.), *International Tables for Crystallography, Vol. C: Mathematical, physical and chemical tables*, 3rd edition, Springer, **2006**.
[18] H. E. Fischer, G. J. Cuello, P. Palleau, D. Feltin, A. C. Barnes, Y. S. Badyal, J. M. Simonson, *Appl. Phys. A Mater. Sci. Process.* **2002**, *S 74* 160–162.
[19] A. Watanabe, G. Kobayashi, N. Matsui, M. Yonemura, A. Kubota, K. Suzuki, M. Hirayama, R. Kanno, *Electrochem. (Tokyo)* **2017**, *85*, 88–92.
[20] N. Matsui, Y. Hinuma, Y. Iwasaki, K. Suzuki, J. Guangzhong, H. Nawaz, Y. Imai, M. Yonemura, M. Hirayama, G. Kobayashi, R. Kanno, *J. Mater. Chem.* **2020**, *A 8*, 24685–24694.
[21] J. P. Vidal, G. Vidal-Valat, *Acta Crystallogr.* **1986**, *B 42*, 131–137.
[22] T. Farley, W. Hayes, S. Hull, M. Hutchings, M. Vrtis, *J. Phys. Condens. Matter* **1991**, *3*, 4761–4781.
[23] R. D. Shannon, *Acta Crystallogr.* **1976**, *A 32*, 751–767.
[24] H. Kohlmann, K. Yvon, *J. Alloys Compd.* **2000**, *299*, L16–L20.
[25] H. Kohlmann, F. Gingl, T. Hansen, K. Yvon, *Angew. Chem. Int. Ed.* **1999**, *38*, 2029–2032; *Angew. Chem.* **1999**,*111*, 2145–2147.
[26] H. Kohlmann, C. Hein, R. Kautenburger, T. C. Hansen, C. Ritter, S. Doyle, *Z. Kristallogr.* **2016**, *231*, 517–523.
[27] H. Bärnighausen, *J. Prakt. Chem.* **1966**, *34*, 1–14.
[28] Ø. S. Fjellvåg, M. Krzystyniak, P. Vajeeston, A. O. Sjåstad, J. Armstrong, *J. Phys. Commun.* **2019**, *3*, 103002 (1–7).
[29] A. J. E. Rowberg, C. G. Van de Walle, *ACS Appl. Energ. Mater.* **2021**, *4*, 6348–6355.

[30] Y. Iwasaki, N. Matsui, K. Suzuki, Y. Hinuma, M. Yonemura, G. Kobayashi, M. Hirayama, I. Tanaka, R. Kanno, *J. Mater. Chem.* **2018**, *A 6*, 23457–23463.
[31] F. Takeiri, A. Watanabe, A. Kuwabara, H. Nawaz, N. I. P. Ayu, M. Yonemura, R. Kanno, G. Kobayashi, *Inorg. Chem.* **2019**, *58*, 4431–4436.
[32] H. W. T. Morgan, H. J. Stroud, N. L. Allan, *Chem. Mater.* **2021**, *33*, 177–185.
[33] a) G. M. Sheldrick, *Software ShelX-2013*, University of Göttingen, **2013**; b) G. M. Sheldrick, *Acta Crystallogr.* **2015**, *C 71*, 3–8.
[34] J. Rodriguez-Carvajal, *Z. Phys. B* **1993**, *192*, 55–69; J. Rodríguez-Carvajal, *IUCr Newsletter* **2001**, *26*, 12–16.
[35] H. E. Fischer, A. C. Barnes, P. S. Salmon, *Rep. Progr. Phys.* **2006**, *69*, 233–299.
[36] a) H. M. Rietveld, *Acta Crystallogr.* **1967**, *22*, 151–152; b) H. M. Rietveld, *J. Appl. Crystallogr.* **1969**, *2*, 65–71.
[37] J. E. Lynn, P. E. Seeger, *Atom. Data Nucl. Data Tables* **1990**, *44*, 191–207.
[38] L. W. Finger, D. E. Cox, A. P. Jephcoat, *J. Appl. Crystallogr.* **1994**, *27*, 892–900.
[39] L. W. Finger, *J. Appl. Crystallogr.* **1998**, *31*, 111.

Manuscript received: August 3, 2022
Revised manuscript received: September 12, 2022

